Scutellaria Extract Inhibits Proliferation and Migration of Brain-Metastatic Lung Cancer Cells via Regulation of Multiple Signaling Pathways

Robert E. Wright III[1Ψ], Lubana Shahin[2Ψ], Venumadhavi Gogineni[1], Zahin Hussain[1], Aroma Naeem[1], Sudha Sadasivan[3], Indrajit Sinha[4], Melody Neely[5], Sharon K. Michellhaugh[6], Sandeep Mittal[6], Nirmal Joshee[2]*, and Prahlad Parajuli[1]*

[1]Department of Oncology, Wayne State University & Karmanos Cancer Institute, Elliman Research Building, # 2230, 423 East Canfield Street, Detroit, MI.
[2]Fort Valley State University, Fort Valley, GA.
[3]Henry Ford Health System, Detroit, MI.
[4]Acenzia Inc., Oldcastle, Ontario, Canada.
[5]Molecular and Biomedical Sciences Dept., University of Maine, Orono, ME.
[6]Department of Neurosurgery, Virginia Polytechnic Institute and State University, Blacksburg, VA, USA
[Ψ]Equal first authors

***Corresponding authors:** pparajuli@med.wayne.edu; josheen@fvsu.edu

Manuscript received: March 6, 2021

Keywords: NSCLC, *Scutellaria,* wogonin, p38 MAPK, metastasis, zebrafish

ABSTRACT

Lung cancer is one of the most lethal solid cancers with a high propensity for brain metastasis. *Scutellaria* spp., a widely used herb in Chinese and Native American medicine, can inhibit the growth of various tumor types, including brain tumors. This study mechanistically evaluated the efficacy of *Scutellaria ocmulgee* leaf (SocL) extract against the proliferation and metastatic potential of brain-metastatic lung cancer cells. Two non-small cell lung cancer (NSCLC) cell lines and two patient-derived brain-metastatic NSCLC cells were used in this study. The proliferation/survival of NSCLC cells was examined via WST assay, while induction of apoptosis was evaluated via flow cytometry. In vivo and in vitro metastatic potential of NSCLC cells were evaluated using a zebrafish model and a wound-healing assay, respectively. Intracellular signaling was queried by western blot analysis. SocL extract and the constituent flavonoid wogonin dose-dependently inhibited the proliferation of NSCLC cells, with 50% inhibition of proliferation at approximately 150 µg/ml. SocL extract dose-dependently enhanced the frequency of early apoptotic cells. There was a dose-dependent inhibition of Akt and p44/42, while the phosphorylation of p38 was dose-dependently enhanced by SocL extract. SocL-mediated inhibition of proliferation and induction of apoptosis was significantly reversed by specific inhibitors of p38 signaling. Finally, the migration/metastatic potential of NSCLC cells was dose-dependently inhibited by SocL extract in vitro as well as in the zebrafish model, which involved modulation of MMP2 expression. Our studies indicate that SocL extract could be a potential candidate for developing neoadjuvant therapy for metastatic NSCLC.

Abbreviations: Akt, protein kinase B; Bcl-2, B-cell lymphoma 2; Bcl-xL, B-cell lymphoma-extra large; DMEM, Dulbecco's Modified Eagle Medium; ERK, extracellular signal-related kinases; FBS, fetal bovine serum; GSK, glycogen synthase kinase; HRP, horseradish peroxidase enzyme; IACUC, Institutional Animal Care and Use Committee; ICIs, immune checkpoint inhibitors; MAPK, mitogen-activated protein kinases; MMPs, Matrix metallopeptidases; NSCLC, non-small cell lung cancer; PBS, phosphate-buffered saline; PFA, paraformaldehyde; PVDF, polyvinylidene difluoride; SocL, *Scutellaria ocmulgee* leaves; TCM,

traditional Chinese medicine; TGF-β1, transforming growth factor beta 1; WST, Water-soluble tetrazolium salt

INTRODUCTION

Lung cancer is one of the most prevalent and lethal cancers with an estimated 228,150 new cases with an estimated mortality of 142,000 in the U.S. in 2019 (Society, 2019). Metastasis is a major concern with advanced forms of lung cancer, with the brain as a frequent site of migration (Tamura et al., 2015). Non-small cell lung cancer (NSCLC) comprises approximately 85% of lung cancers. Sub-types of NSCLC include adenocarcinoma, squamous cell carcinoma, and large cell carcinoma (American Cancer Society, 2019). Adenocarcinoma is the most prevalent form of metastatic lung cancer with an overall 5-year survival rate of 19.4% in treated patients, and 2% in those who wish to forgo treatment. Immunotherapy, specifically the use of immune checkpoint inhibitors (ICIs), has significantly improved clinical outcomes in patients with lung adenocarcinoma. However, most lung cancer patients do not respond to ICIs or develop resistance after the initial response (Milovanovic et al., 2017; Institute, 2019). Therefore, it is necessary to develop novel forms of neoadjuvant therapeutics for this deadly disease.

Previous research from our lab has shown that the leaf extract of *Scutellaria ocmulgee* (SocL) can inhibit the growth of various tumor types, including malignant gliomas, via direct tumor-cytotoxic activity (Parajuli et al., 2009; Parajuli et al., 2011) as well as via modulation of stromal immune functions (Dandawate et al., 2012). In this study, we determined inhibition of the brain-metastatic potential of lung cancer cells by SocL extract in vitro as well as in vivo using a zebrafish model. Some underlying mechanisms in relation to modulation of p38 MAPK signaling were also examined.

MATERIALS AND METHODS

Scutellaria ocmulgee leaf (SocL) extract and wogonin. Cultivation of *S. ocmulgee* plants, harvesting of leaves, and extraction were performed as per the protocol described earlier (Parajuli et al., 2009). Plants were cultivated in the greenhouse conditions to minimize batch-to-batch variation. New plants were established through root divisions in March that reach maturity in May and leaves were harvested before the onset of flowering. The leaves were dried with constant turning in shed at room temperature to remove about 80% moisture. The dried leaves were then crushed and processed for methanol:water (1:1) extraction using an ASE apparatus (Dionex Corporation, Sunnyvale, CA), as described earlier (Parajuli et al., 2009). The extract has been characterized and tested for anti-cancer activity against U87-MG glioma cell line and wogonin was used as an internal standard as described previously (Parajuli et al., 2009; Parajuli et al., 2011). The flavonoid wogonin (purity 98%) was purchased from Sigma Chemical Co. (St. Louis, MO). Wogonin was reconstituted in dimethyl sulfoxide (DMSO) and then diluted in appropriate media, as indicated. The final concentration of DMSO in the media for all experiments were <0.1%. Therefore, 0.1% DMSO was used in the Control media for all experiments.

Lung cancer cells. Two standardized metastatic non-small cell lung cancer lines, A-549 and NCI-H358 (obtained from American Type, Tissue Culture, Manassas, VA) and two patient-derived brain metastatic lung AC cells, 18-032 and 18-033 were used in this study (see Supplementary Material for redacted pathological reports). Tumor tissues were obtained from patients with histologically-confirmed brain-metastatic lung cancer immediately after surgical resection, under a protocol approved by the Institutional Review Board at Wayne State University (IRB # 111610MP2E). Dissociation and culture of patient-derived tumor cells were performed following a previously described method (Michelhaugh et al., 2015; Parajuli et al., 2016). The tumor cells were cultured in DMEM/F12 containing 10% FBS.

Proliferation assay. A previously described method was followed (Parajuli et al., 2016) with some modifications. Briefly, cells were seeded in 96-well flat-bottom plates (2 x10^4 cells/well) and cultured in the presence of varying doses of SocL and specific cell signaling inhibitors, as indicated. After incubation at 37°C for 3 days, cell viability was evaluated using the WST-1 assay kit (Clonetech Laboratories, Mountain View, CA) as per the manufacturer's protocol. Cell viability/proliferation was expressed as a percent of control (cells cultured with medium alone).

Apoptosis assay. A previously described method was followed (Parajuli et al., 2009) with some

modifications. Briefly, cells were seeded in 6-well flat-bottom plates (5 x10^5 cells/well) and cultured in the presence of varying doses of SocL and specific cell signaling inhibitors, as indicated. After incubation at 37°C for 48 h, the cells were stained with Annexin V-FITC and PI, then analyzed via flow cytometry.

Intracellular signaling analysis via western blot assay. A previously described method was followed (Dandawate et al., 2012). Briefly, lung cancer cells were seeded in 6- or 12-well plates and cultured in the presence of varying doses of SocL, as indicated. After incubation at 37°C for 48 h, cells were lysed, 20–30 µg aliquots of total protein were electrophoresed, transferred onto a polyvinylidene difluoride (PVDF) membrane, and probed with specific antibodies (Table 1S, under Supporting Information section). Detection of HRP-conjugated secondary Abs was performed using SuperSignal (Pierce, Rockford, IL) and chemiluminescence was recorded using an Omega imaging system (UltraLum Inc., Claremont, CA) as per manufacturer's instructions. β-actin was used as the loading control. The density of protein bands was quantified using ImageJ software.

Zebrafish tumor transplantation model. The study was performed as per the protocol approved by the Institutional Animal Care and Use Committee (IACUC) of Wayne State University (Protocol # A 10-06-12). The pigment mutant (Casper) strains of Zebrafish (*Danio rerio*) were raised, staged, and maintained according to standard procedures. A published protocol was followed for tumor transplantation (Drabsch et al., 2013). Briefly, dechorionated 2 days-post fertilization (dpf) zebrafish embryos were anesthetized with 0.003% tricaine (Sigma-Aldrich, St. Louis, Mo) and positioned in a 10-cm Petri dish coated with 3% agarose (see Supporting Information, Figure 1S for a schematic representation of the in vivo protocol). Tumor cells were labeled with the fluorescent cell tracker CM-DiI (Invitrogen, Waltham, MA) following standard protocol and suspended in PBS containing 25 µM glucose and 0.2% gelatin. The cell suspension was loaded into borosilicate glass capillary needles (1 mm O.D. × 0.78 mm I.D.; Harvard Apparatus) and the injections were performed using a Picolitre Injector and a manipulator (Harvard Apparatus, Holliston, MA). Approximately 200 cells were implanted into the yolk sac in 13.2 nl volume. After implantation with mammalian cells, zebrafish embryos (including PBS-injected controls) were maintained at 33°C. Two to four hours after tumor implantation, the embryos were divided into experimental groups and 'seeded' by placing 10 embryos/well into a 6-well plate in 4 ml E3 water. Plant extract (SocL) was added into the water at various doses, as indicated. After further incubating for 4 days, the embryos were euthanized with 0.03% tricaine, fixed with 4% PFA and whole mounted on a slide for imaging via confocal microscopy (Zeiss LSM 780). Quantification of fluorescence was performed in ImageJ. Images were imported and a threshold image was created from the red color channel. A total pixel count within the yolk sac or outside the yolk sac, including in the brain (metastasis) was enumerated using the measuring functionality within ImageJ. Values from single cells imaged at the same resolution (approximately 5-pixel count corresponded to one cell volume) were used to estimate the number of tumor cells at the injection site (yolk sac) and in the brain area.

Wound-healing/ Scratch assay. Cells were seeded in 12-well plates (2.5 x 10^5 cells/well) and incubated in DMEM/F12 containing 10% FBS for 24-48 h, until approximately 80% confluency. Cells were then linearly scratched with the tip of a 200 µL pipette and subsequently incubated with different doses of SocL extract. Images were captured under a microscope (Olympus) using QCapture Pro (Teledyne QImaging) at various time points, as indicated. Images were analyzed using ImageJ (NIH, Bethesda, MD).

Statistical analysis. All the experiments were performed three times with at least two different NSCLC cell types. Statistical significance was determined using one-way ANOVA followed by a post hoc t-test to compare pairs of samples. A 'p' value of less than 0.05 was considered significant**.**

RESULTS

First, we examined the dose-dependent effect of SocL extract on the proliferation and apoptosis of lung cancer cells. Two NSCLC cell lines, A-549 and NCI-H358, as well as two patient-derived, brain-metastatic lung cancer cells 18-032 and 18-033, were cultured for 72 h in the presence of various doses of SocL extract or flavonoid wogonin. As analyzed via WST-1 assay, SocL extract dose-dependently

inhibited the proliferation/viability of all NSCLC cells tested, with 50% inhibition of proliferation (IC_{50}) at a dose of approximately 150 µg/ml (Fig. 1A).

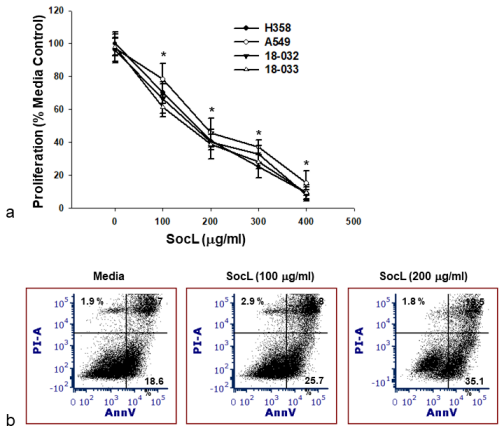

Figure 1. SocL inhibits proliferation and enhances apoptosis in non-small cell lung cancer (NSCLC) cells. Two NSCLC cell lines (A549 and H358) and two patient-derived, brain metastatic NSCLC cells (18-032 and 18-033) were cultured with various doses of SocL extract, as indicated. (A) After 72 hours of culture, a WST-1 assay was performed to estimate cell proliferation/viability as described under the Methods. WST-1 assay was performed in triplicates with three repeats (B) After 48 hours of culture, cells were stained with Annexin-V and PI then analyzed by flow cytometry. Apoptosis data (dot plots) are representative of two different experiments performed in duplicates (n=4) with two different NSCLC cells with similar results. *p<0.05 versus media controls.

SocL extract has previously been characterized by HPLC for the presence of 6 major flavonoids (apigenin, baicalein, baicalin, chrysin, scutellarein and wogonin) and only wogonin was detectable in trace amounts (0.1 µg/mg extract) (Parajuli et al., 2009). Similar to the crude SocL extract, wogonin also dose-dependently inhibited the proliferation of H358 and 18-032 cells, with an IC_{50} value at approximately 50 µM dose (Supporting Information, Figure 2S).

Cells (NSCLC) were similarly cultured with various doses of SocL extract for 48 h and induction of apoptosis was analyzed as described in the methods section. SocL extract dose-dependently enhanced the frequency of early apoptotic cells (25.7% and 35.1% Annexin-V positive cells at doses 100- and 200 µg/ml, respectively) compared to the controls (18.6%) (Fig. 1B, representative results from 18-032 cells). Similar results were obtained with H358 cells (data not shown).

To explore possible mechanisms associated with the inhibition of proliferation and promotion of apoptosis, NSCLC cells were cultured with various doses of SocL extract for 48 h, and intracellular signaling activity was analyzed via western blot assay as described under the methods section. We observed baseline constitutive activation (phosphorylation) of Akt (PI3 kinase) and p44/42 (MAPK) pathways in all NSCLC cells tested. Representative data of 18-032 cells is shown in Fig. 2. There was a dose-dependent inhibition of phosphorylated Akt and p44/42 following treatment with SocL extract (Fig. 2A and 2B). On the other hand, phosphorylation of p38 was dose-dependently enhanced following treatment with SocL extract (Fig. 2C).

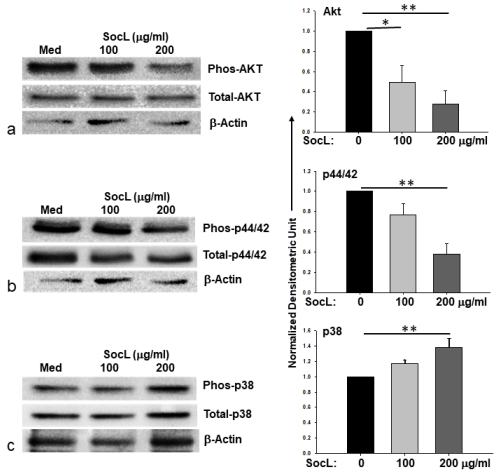

Figure 2. Modulation of various cell signaling pathways by SocL in NSCLC cells. NSCLC cells were cultured with various doses of SocL extract, as indicated. After 48 hours, cells were lysed, electrophoresed and analyzed by western blot assay, as described in the Methods section. Images for phosphorylated and non-phosphorylated proteins for (A) Akt, (B) p44/42 ERK and (C) p38 MAPK, as well as corresponding b-actin images, were quantitated by ImageJ software to obtain densitometric values. Histogram plots represent data for phosphorylated proteins, which are normalized against values for β-actin. *p<0.05 versus media controls. Data are mean ± SD of three different experiments. (A) *p = 0.035; **p = 0.011; (B) **p = 0.009; (C) **p = 0.032.

The expression of apoptosis-regulating proteins Bcl-2 and Bcl-xL were also analyzed under similar conditions. We observed dose-dependent inhibition of both Bcl-2 and Bcl-xL by SocL extract (Fig. 3). However, only inhibition of Bcl-xL (approximately 40% and 60% inhibition by SocL at doses 100- and 200 µg/ml, respectively) was statistically significant (Fig. 3).

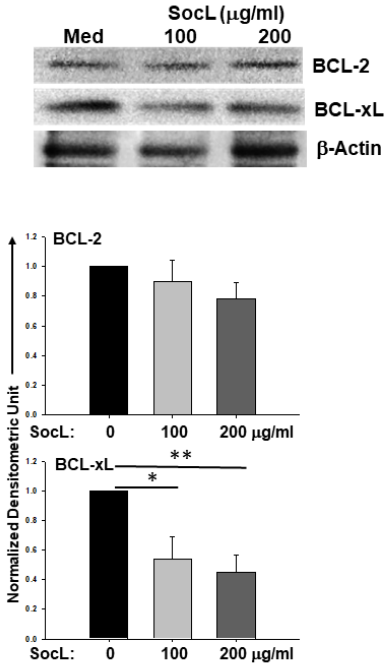

Figure 3. Modulation of apoptosis-regulating proteins by SocL in NSCLC cells. NSCLC cells were cultured with various doses of SocL extract, as indicated. After 48 hours, cells were lysed, electrophoresed and analyzed by western blot assay, as described in the Methods section. Images for expression of (A) Bcl-2 and (B) Bcl-xL proteins were quantitated by ImageJ software to obtain densitometric values. Histogram plots represent data for (A) Bcl-2 and (B) Bcl-xL proteins, which are normalized against corresponding values for β-actin. Data are mean ± SD of three different experiments. (B) *p = 0.034; **p = 0.015

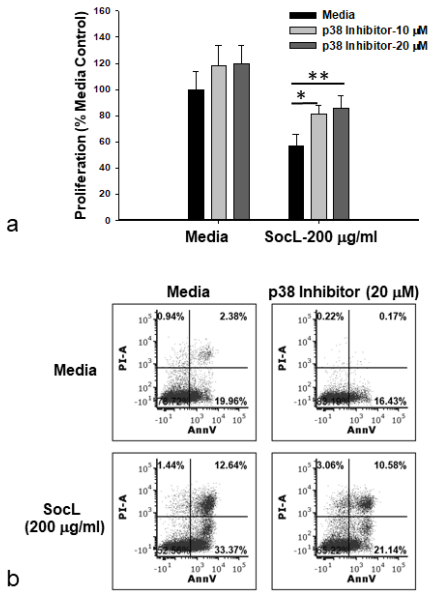

Figure 4. Inhibition of proliferation and induction of apoptosis by SocL is partially mediated via modulation of p38 MAPK signaling. The patient-derived, brain metastatic NSCLC cells (18-032 and 18-033) were cultured with SocL extract in the presence of various doses of specific p38 inhibitor SB 202190, as indicated. (A) After 72 hours of culture, a WST-1 assay was performed to estimate cell proliferation/viability as described under the methods. Data are mean ± SD of one experiment (n=3), out of two performed with similar results. *p = 0.024; **p = 0.017. (B) After 48 hours of culture, cells were stained with Annexin-V and PI then analyzed by flow cytometry to estimate the induction of apoptosis. Apoptosis data (dot plots) are representative of two different experiments performed with 18-032 cells. Experiments were repeated with 18-033 cells with similar results.

In our previous study, SocL upregulated the activation of p38 MAPK in glioma cells (Dandawate et al., 2012). Data shown in Fig. 2C also displayed similar dose-dependent increase in p38 activation by SocL in lung cancer cells. We, therefore, wanted to further examine whether the activation of p38 played a role in the inhibition of proliferation and induction of apoptosis by SocL. As shown in Fig. 4A, NSCLC cells treated with SocL showed an expected decrease in proliferation, which was dose-dependently reversed by the specific p38 inhibitor (SB 202190, Sigma-Aldrich). Similarly, SocL-induced apoptosis was also significantly reversed by SB202190 (21.14% versus 33.37% in the SocL group) (Fig. 4B). These results indicated that SocL-mediated enhancement of p38 activation is partially involved in the inhibition of proliferation and induction of apoptosis in NSCLC cells.

Finally, inhibition of migration and metastasis of NSCLC cells by SocL extract were examined in vitro and in vivo, along with any modulation in MMP2/MMP9 expression. A zebrafish model was utilized to examine the effects of SocL in vivo, as described in the methods section. Briefly, zebrafish embryos were inoculated with approximately 200 DiI (red fluorescent) -tagged H358 cells into the yolk sacs, then treated with SocL extract (200 μg/ml in E3 water) or E3 water alone (control). The zebrafish embryos were further incubated for 96 h, euthanized, and then imaged under a confocal microscope. The proliferation of injected NSCLC cells, as well as noticeable cell migration to the brain, was observed in the control group (Fig. 5). On the other hand, SocL treated zebrafish embryos had significantly lower

cell volume in the yolk sac while migration into the brain area was not noticeable (Fig. 5).

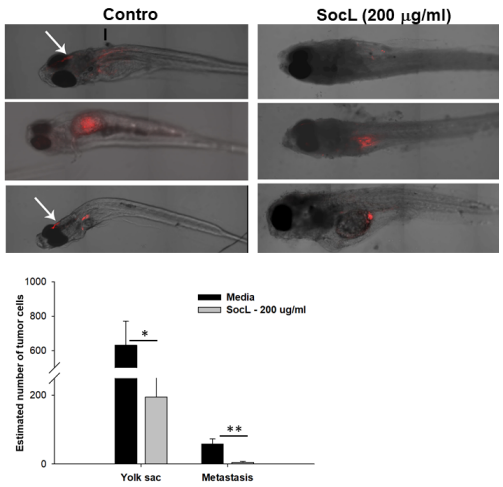

Figure 5. Inhibition of brain metastasis of NSCLC cells by SocL in a zebrafish model. A zebrafish model of brain metastatic NSCLC was developed, as described in the Methods section. Briefly, metastatic NSCLC (H358) cells were labeled with a red fluorescent dye (Dil) and approximately 200 cells were nano-injected into the yolk sacs of 48 hpf zebrafish embryos. The embryos were then incubated in E3 water containing SocL extract, as indicated. After 72 hours, images were taken under a confocal microscope. The images were analyzed by Zen Lite software and the red fluorescence intensity (pixels as a measure of cell volume) was quantitated using ImageJ. Data are mean ± SD of one experiment (n=10), out of two performed with similar results. *p = 0.009; **p = 0.001.

To further test what effects SocL has on cell migration, a scratch assay was performed as described in the Methods section. Images were taken before and after treatment to record the progression of wound-healing. We observed that control wells displayed widespread cell migration, with cells interspersed within the initial scratch (Fig. 6). SocL treated wells showed a marked decrease in migration, and in the case of 200 μg/ml, a slight digression occurred as measured by a comparison of the area of the scratch before and after treatment, indicating inhibition of cell survival/proliferation by SocL extract (Fig. 6). The results display a clear dose-dependent inhibition of migration or pro-metastatic behavior of NSCLC cells by SocL extract.

Matrix-metallopeptidases (MMPs) contribute greatly to both migration and metastasis, with metastatic cancer cells producing elevated levels of MMPs (Gialeli, Theocharis et al. 2011).

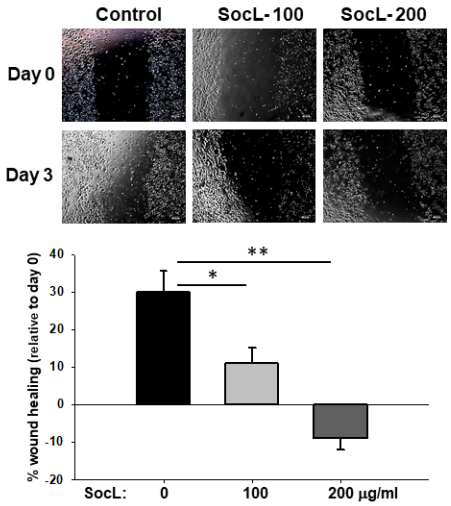

Figure 6. Inhibition of in vitro migration of NSCLC cells by SocL extract. NSCLC cells were plated in 12 well plates and a scratch/wound-healing assay was performed, as described in the Methods section. Briefly, a straight-line scratch/wound was made in the middle of the semi-confluent monolayer of cells. The cells were cultured with various doses of SocL, as indicated, for 72 hours. Images were taken before treatment (day 0), as well as after 72 hours (day 3). The scratch areas were quantitated using ImageJ software. The histogram plot represents the scratch area on day 3 as a % value of the exact same scratch on day 0. Data are mean ± SD of one experiment (n=3), out of two performed with similar results. *p = 0.012; **p = 0.002.

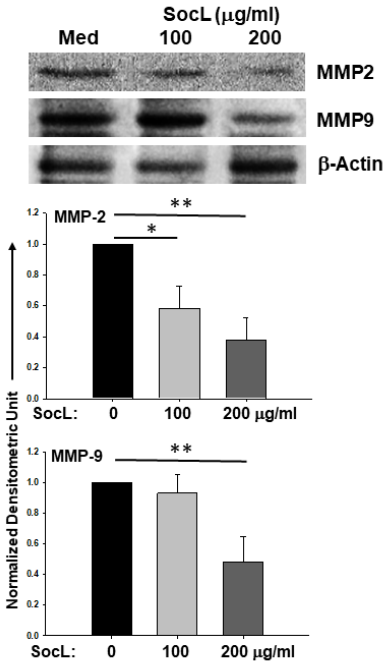

Figure 7. Modulation of migration/metastasis-regulating proteins by SocL in NSCLC cells. NSCLC cells were cultured with various doses of SocL extract, as indicated. After 48 hours, cells were lysed, electrophoresed and

analyzed by western blot assay, as described in the Methods section. Images for expression of (A) MMP2 and (B) MMP9 proteins were quantitated by ImageJ software to obtain densitometric values. Histogram plots represent data for (A) MMP2 and (B) MMP9 proteins, which are normalized against corresponding values for β-actin. Data are mean ± SD of three different experiments. (A) *p = 0.04; **p = 0.017; (B) **p = 0.034.

We observed a significant, dose-dependent inhibition of MMP2 expression in NSCLC cells following treatment with SocL (40% and 60% inhibition with SocL at 100- and 200 μg/ml, respectively), compared to the control group (Fig. 7A). On the other hand, the greatest drop (45% inhibition compared to control) in MMP9 expression was observed in the higher, 200 μg/ml dose group, while the lower, 100 ug/ml dose showed negligible effects on MMP9 expression (Fig. 7B).

DISCUSSION

Scutellaria is a member of the mint family which has been featured prominently in traditional Chinese medicine (TCM) as well as in Native American folk medicine. Various species of Scutellaria have reported usage for a myriad of ailments including inflammatory disorders, anxiety, and cancer (Patel et al., 2013; Wright and Parajuli, 2019). Our group has previously reported anti-cancer activities of leaf, root, and stem extracts derived from 13 different species of Scutellaria using in vitro models of breast cancer, prostate cancer, and brain cancer (glioma) cells, from which *Scutellaria ocmulgee* Leaf (SocL) extract, containing trace amounts of wogonin, was selected to be the one with most anti-cancer activities (Parajuli et al., 2009). Subsequent work in our lab has used in vitro and in vivo syngeneic models of malignant gliomas and showed that apart from directly interfering with tumor survival and apoptotic pathways in cancer, SocL extracts can modulate the stromal immune component by affecting the TGF-β1 pathway (Parajuli et al., 2011; Dandawate et al., 2012).

Our results indicated that SocL extract could inhibit proliferation, induce apoptosis and inhibit migration/invasion of metastatic lung cancer cells involving the modulation of Akt, P44/42, and p38 signaling pathways. *Scutellaria barbata* extracts have been shown to inhibit metastasis/migration of colorectal cancer cells, likely via targeting the two signaling pathways PI3 kinase/Akt and TGF-β/Smad3 (Jin et al., 2017). One of the Scutellaria flavonoids, baicalin has recently been shown to inhibit invasion, migration, and metastasis of breast cancer cells via modulation of p38 MAPK activity (Xiu- Feng et al., 2013). In another recent study, *Scutellaria barbata* extract inhibited proliferation, induced autophagy, and apoptosis in CL1-5 Lung cancer cells via inhibition of p38 MAPK signaling (Chen et al., 2017). Baicalein has been reported to induce apoptosis in FRO thyroid cancer cells via upregulation of P38 and modulation of AKT pathways (Han et al., 2019). The results of these studies agree with the results of our studies on SocL extract. Our previous studies have also shown in vitro and in vivo anti-tumor activity of SocL extract via modulation of Akt/GSK-3b and p44/42 ERK signaling in malignant glioma cells (Parajuli et al., 2009, Parajuli et al., 2011). As reported earlier, wogonin was detected in SocL extract only in very small amounts (0.1 μg/mg extract), which does not correlate with the cytotoxic activity of the extract. This suggests that wogonin has synergistic activity with other phytochemicals in the extract which are yet to be identified. Our group has been working on further identifying the active components in the extract via HPLC/MS fractionation and in vitro characterization.

Protein Kinase B, also known as Akt, can play an important role in modulating proliferation, apoptosis as well as metastatic behavior of cancer cells (Cheung and Testa, 2013). Constitutive activation of the Akt pathway is common in many cancers and can result in uncontrollable cell proliferation and migration (Tian et al., 2018). Inhibition of Akt combined with activation of p38 MAPK, as observed in the current study, is associated with the anti-proliferative and pro-apoptotic activity (Berra et al., 1998).

P44/42, also known as extracellular signal-regulated kinase 1/2 (ERK1/2), is known to promote cellular proliferation and is a common pathway upregulated in various cancers (Rodriguez-Berriguete et al., 2012). P44/42 MAPK might also play a role in the production of MMP2. In a study identifying the role of MMP2 in brain metastatic breast cancer, higher levels of Erk1/2 activation were found to correlate with heightened levels of MMP2 (Mendes et al., 2007). The dose-dependent inhibition of both MMP2 and P44/42 activation by SocL, as observed in the current study, could be explained by an analogous mechanism, though more investigation is needed to formulate a concrete link.

P38 MAP kinase is a stress response protein associated with promoting apoptosis in certain cell types via inhibition of Bcl-2 (Cai et al., 2006). In fact p38 MAPK signaling can have either agonistic or antagonistic effect on tumor cell survival, proliferation or migration, depending on the tumor type and interaction with other signaling activities. Therefore, the tumor type and context of signaling activities should be carefully considered while designing therapeutic strategies targeting the intracellular signaling pathways. In our previous study, SocL and flavonoids found in SocL had been associated with an increase in the phosphorylation of p38 (Dandawate et al., 2012). The Bcl-2 and its family members are associated with anti-apoptotic effects and are commonly upregulated in many cancers (Frenzel et al., 2009). Although in the current study, the modulation of BCL-2 by SocL was very marginal, a significant decrease in BCL-xL was observed in NSCLC cells, providing insight on how apoptosis might be regulated after SocL treatment.

We have previously reported in vivo activity of SocL extract against malignant gliomas without apparent toxicity at a peroral dose of 250 mg/kg (Parajuli et al., 2011). Some clinical studies have shown promising signs for other species of Scutellaria in cancer treatment applications. In a phase 1b dose-escalation clinical trial, in patients with metastatic breast cancer, treatment with *Scutellaria barbata* displayed encouraging safety and efficacy (Perez et al., 2010). Lin et al. (2019) have recently published a retrospective study evaluating the risk of lung cancer development in more than 34,000 patients with chronic obstructive pulmonary disease (COPD) among users (11,180) and non-users (23,319) of Chinese herbal medicine (CHM), of which Scutellaria was one of the top 10 components. The result indicated that patients with COPD who used CHM in combination with conventional therapies had a significantly lower risk of lung cancer development compared to the patients not using CHM (Lin et al., 2019).

Treatment for lung cancer can vary depending on type and stage but most include the typical chemo- and radiation therapies. Many of these treatments, especially platinum-based therapies, are also associated with known adverse side effects. Moreover, survival rates substantially decrease once metastasis has occurred (Poullis et al., 2014). Therefore, any non-deleterious treatment with anti-metastatic activity could potentially improve the survival rate in these patients.

Finally, few studies have focused on the direct effects of Scutellaria on metastasis. Gong et al. (2014) investigated the effects of flavonoids baicalin, baicalein and wogonin found in *Scutellaria baicalensis* on lung cancer metastasis, proliferation, and inflammation induced by nicotine. The results were very promising. Zheng et al. (2018) studied the effects of *Scutellaria barbata* on bone metastatic breast cancer and have reported inhibition of metastasis and cell viability via modulation of RANKL (Zheng et al., 2018). We have observed a dose-dependent inhibition of metastatic behavior of brain metastatic NSCLC both in vitro and in a zebrafish model by direct treatment with SocL. The results indicate a promise for *Scutellaria ocmulgee* as a potential anti-metastatic agent that could be used in future combination therapy.

ACKNOWLEDGMENTS

Our institutional Microscopy, Imaging, and Cytometry Resources (MICR) core facility were used for the flow cytometry studies. The Core is supported, in part, by NIH Center grant P30 CA22453 to the Karmanos Cancer Institute, Wayne State University, and the Perinatology Research Branch of the National Institutes of Child Health and Development. We thank Evans Allen grant (USDA NIFA) GEOX 5220 (PI N. Joshee) for supporting LS to conduct part of the research at Wayne State University.

REFERENCES

Berra, E., Diaz-Meco, M. a. T., and Moscat, J. 1998. The activation of p38 and apoptosis by the inhibition of Erk is antagonized by the phosphoinositide 3-kinase/Akt pathway. J. Biological Chemistry 273(17): 10792-10797.

Cai, B., Chang, S. H., Becker, E. B. E., Bonni, A., and Xia, Z. 2006. p38 MAP kinase mediates apoptosis through phosphorylation of BimELat Ser-65. J. Biological Chemistry 281(35): 25215-25222.

Chen, C.-C., Kao, C.-P., Chiu, M.-M., and Wang, S.-H. 2017. The anti-cancer effects and mechanisms of *Scutellaria barbata* D. Don on CL1-5 lung cancer cells. Oncotarget 8(65): 109340-109357.

Cheung, M. and Testa, J.R. 2013. Diverse mechanisms of AKT pathway activation in human malignancy. Current Cancer Drug Targets 13(3): 234-244.

Dandawate, S., Williams, L., Joshee, N., Rimando, A.M., Mittal, S., Thakur, A., Lum, L. G., and Parajuli, P. 2012. Scutellaria extract and wogonin inhibit tumor-mediated induction of T(reg) cells via inhibition of TGF-β1 activity. Cancer Immunology, Immunotherapy 61(5): 701-711.

Drabsch, Y., He, S., Zhang, L., Snaar-Jagalska, B.E., and ten Dijke, P. 2013. Transforming growth factor-beta signalling controls human breast cancer metastasis in a zebrafish xenograft model. Breast Cancer Res 15(6): R106.

Frenzel, A., Grespi, F., Chmelewskij, W., and Villunger, A. 2009. Bcl2 family proteins in carcinogenesis and the treatment of cancer. Apoptosis 14(4): 584-596.

Gialeli, C., Theocharis, A.D., and Karamanos, N.K. 2011. Roles of matrix metalloproteinases in cancer progression and their pharmacological targeting. FEBS J 278(1): 16-27.

Gong, W.-Y., Wu, J.-F., Liu, B.-J., Zhang, H.-Y., Cao, Y.-X., Sun, J., Lv, Y.-B., Wu, X., and Dong, J.-C. 2014. Flavonoid components in *Scutellaria baicalensis* inhibit nicotine-induced proliferation, metastasis and lung cancer-associated inflammation in vitro. International J. Oncology 44(5): 1561-1570.

Han, S. E., Park, C.H., Nam-Goong, I.S., Kim, Y.I., and Kim, E.S. 2019. Anticancer effects of baicalein in FRO thyroid cancer cells through the up-regulation of ERK/p38 MAPK and Akt pathway. In Vivo 33(2): 375-382.

Institute, N. C. 2019. Cancer Stat Facts: Lung and Bronchus Cancer, from https://seer.cancer.gov/statfacts/html/lungb.html

Jin, Y., Chen, W., Yang, H., Yan, Z., Lai, Z., Feng, J., Peng, J., and Lin, J. 2017. *Scutellaria barbata* D. Don inhibits migration and invasion of colorectal cancer cells via suppression of PI3K/AKT and TGF-β/Smad signaling pathways. Experimental and Therapeutic Medicine 14(6): 5527-5534.

Lin, T.-H., Chen, S.-I., Su, Y.-C., Lin, M.-C., Lin, H.-J., and Huang, S.-T. 2019. Conventional western treatment combined with chinese herbal medicine alleviates the progressive risk of lung cancer in patients with chronic obstructive pulmonary disease: a nationwide retrospective cohort study. Front. Pharmacol. 10: 987-987.

Mendes, O., Kim, H.-T., Lungu, G., and Stoica, G. 2007. MMP2 role in breast cancer brain metastasis development and its regulation by TIMP2 and ERK1/2. Clinical and Experimental Metastasis 24(5): 341-351.

Michelhaugh, S. K., Guastella, A.R., Varadarajan, K., Klinger, N.V., Parajuli, P., Ahmad, A., Sethi, S., Aboukameel, A., Kiousis, S., Zitron, I.M., Ebrahim, S.A., Polin, L.A., Sarkar, F.H., Bollig-Fischer, A., and Mittal, S. 2015. Development of patient-derived xenograft models from a spontaneously immortal low-grade meningioma cell line, KCI-MENG1. J Transl Med 13: 227.

Milovanovic, I. S., Stjepanovic M., and Mitrovic, D. 2017. Distribution patterns of the metastases of the lung carcinoma in relation to histological type of the primary tumor: An autopsy study. Annals of Thoracic Medicine 12(3): 191-198.

Parajuli, P., Anand, R., Mandalaparty, C., Suryadevara, R., Sriranga, P. U., Michelhaugh, S.K., Cazacu, S., Finniss, S., Thakur, A., Lum, L. G., Schalk, D., Brodie, C., and Mittal, S. 2016. Preferential expression of functional IL-17R in glioma stem cells: potential role in self-renewal. Oncotarget 7(5): 6121-6135.

Parajuli, P., Joshee, N., Chinni, S.R., Rimando, A.M., Mittal, S., Sethi, S., and Yadav, A.K. 2011. Delayed growth of glioma by Scutellaria flavonoids involve inhibition of Akt, GSK-3 and NF-κB signaling. Journal of Neuro-Oncology 101(1): 15-24.

Parajuli, P., Joshee, N., Rimando, A.M., Mittal, S., and Yadav, A.K. 2009. In vitro antitumor mechanisms of various Scutellaria extracts and constituent flavonoids. Planta Med 75(01): 41-48.

Patel, P., Joshee, N., Mittal, S., and Parajuli, P. 2013. Anti-cancer mechanisms of wogonin and related Scutellaria flavonoids. Curr Cancer Ther Rev 9: 34-42.

Perez, A. T., Arun, B., Tripathy, D., Tagliaferri, M.A., Shaw, H.S., Kimmick, G.G., Cohen, I., Shtivelman, E., Caygill, K.A., Grady, D., Schactman, M., and Shapiro, C.L. 2010. A phase 1B dose escalation trial of *Scutellaria barbata* (BZL101) for patients with metastatic breast cancer. Breast Cancer Res Treat 120(1): 111-118.

Poullis, M., Shackcloth, M., Page, R., Asanti-Siaw, J., Woolley, S., and Mediratta, N. 2014. Metastatic index of non-small-cell lung cancer and long-term survival. Asian Cardiovascular and Thoracic Annals 23(2): 185-190.

Rodriguez-Berriguete, G., Fraile, B., Martinez-Onsurbe, P., Olmedilla, G., Paniagua, R., and Royuela, M. 2012. MAP kinases and prostate cancer. J Signal Transduct 2012: 1-9 169170.

Society, A. C. 2019. Key Statistics for Lung Cancer. from https://www.cancer.org/cancer/non-small-cell-lung-cancer/about/key-statistics.html.

Tamura, T., Kurishima, K., Nakazawa, K., Kagohashi, K., Ishikawa, H., Satoh, H., and Hizawa, N. 2015. Specific organ metastases and survival in metastatic non-small-cell lung cancer. Molecular and Clinical Oncology 3(1): 217-221.

Tian, T., Sun, J., Wang, J., Liu, Y., and Liu, H. 2018. Isoliquiritigenin inhibits cell proliferation and migration through the PI3K/AKT signaling pathway in A549 lung cancer cells. Oncology Letters 16(5): 6133-6139.

Wagner, E. F., and Nebreda, A.R. 2009. Signal integration by JNK and p38 MAPK pathways in cancer development.Nature Reviews Cancer **9:**537–549.

Wright, R., and Parajuli, P. 2019. Modulation of tumor immunity by medicinal plant or functional food derived compounds. Medicinal Plants: from Farm to Pharmacy. N. Joshee, S. Dhekney and P. Parajuli (editors). USA, Springer Nature: 275-290.

Xiu- Feng, W., Qian- Mei, Z., Jia, D., Hui, Z., Yi-Yu, L., and Shi- Bing, S. 2013. Baicalin suppresses migration, invasion and metastasis of breast cancer via p38MAPK signaling pathway. Anti-Cancer Agents in Medicinal Chemistry 13(6): 923-931.

Zheng, X., W. Kang, H. Liu and S. Guo. 2018. Inhibition effects of total flavonoids from *Scutellaria barbata* D. Don on human breast carcinoma bone metastasis via downregulating PTHrP pathway. International J. Molecular Medicine 41(6): 3137-3146.